crystals

MDPI

Article

The Effect of Template Reset Operation on the Number of Crystals Precipitated at the Air–Solution Template Interface

Bolor-Uyanga Tumurbaatar, Shuntaro Amari and Hiroshi Takiyama *

Department of Chemical Engineering, Tokyo University of Agriculture and Technology, 24-16, Nakacho-2, Koganei, Tokyo 184-8588, Japan
* Correspondence: htakiyam@cc.tuat.ac.jp

Abstract: The application of template crystallization to developing novel crystalline materials has attracted attention. However, when the air–solution interface becomes the template interface and the target material crystallizes, new nucleation at the template interface is prevented, which is predicted to prevent the increase in the total number of crystals. In this study, we investigated the effect of operations that change the driving force at the air–solution template interface on the number of crystals at the interface. The number of crystals precipitated by changing the local supersaturation was investigated by a novel "template reset" operation, in which the concentration driving force near the template interface is changed by dissolving the crystals at the interface, once precipitated. The results showed that the number of crystals increased significantly after the template reset operation, and the particle size distribution was also improved. The temperature of the solution near the interface after the template reset operation was higher than that of the solution at the bottom of the petri dish and the prepared saturated solution, suggesting that the driving force of crystallization was higher.

Keywords: template crystallization; air–solution interface; number of crystals; local supersaturation; crystal dissolution

check for updates

Citation: Tumurbaatar, B.-U.; Amari, S.; Takiyama, H. The Effect of Template Reset Operation on the Number of Crystals Precipitated at the Air–Solution Template Interface. *Crystals* **2024**, *14*, 591. https://doi.org/10.3390/cryst14070591

Academic Editor: Petros Koutsoukos

Received: 10 June 2024
Revised: 24 June 2024
Accepted: 26 June 2024
Published: 27 June 2024

Copyright: © 2024 by the authors. Licensee MDPI, Basel, Switzerland. This article is an open access article distributed under the terms and conditions of the Creative Commons Attribution (CC BY) license (https://creativecommons.org/licenses/by/4.0/).

1. Introduction

In recent years, many studies have been conducted to develop novel crystalline materials by applying template crystallization to various materials [1–9]. Template crystallization is a technique in which crystals of a target material are precipitated at the template interface using the template material. It has been investigated and is applied to a wide range of fields, such as active pharmaceutical ingredients [10–12], minerals [13–15], and semiconductors [16–18]. Furthermore, in combination with antisolvent crystallization [8,11], the molten salt method [17], and confinement [10,16], the use of the template interface expands the attainability of crystallization operation. One of the key features of template crystallization is the constraint of the nucleation field because of the preferential appearance of crystals at the template interface by the interaction between the template material and the target material [19]. There are various classifications of template materials, divided into soft templates (biomolecules and surfactants) and hard templates (porous silica and silica), according to the template's properties [20]. One of the materials that can act as soft templates are polymers, and it has been reported that micelles of nanometric size formed by copolymers can act as soft templates for gold nanoparticle synthesis [21]. Gold nanoparticles can be distributed homogeneously inside whole micelles or on the peripheral surfaces of polymer particles. Previous studies using gas microbubbles as the soft template concluded that the protein crystallization process consists of three stages: adsorption of the protein on the gas–liquid interface, nucleation on the gas–liquid–solid interface, and crystal growth on the gas–solid interface [22]. Additionally, with different gases of equal concentrations, the proportion of crystals on the bubbles differed and the total number of

crystals followed the same trend as the solubility and polarizability of the gases. Yamamoto et al. reported that when glycine crystals precipitate at the air–solution interface, the formation of a new template interface in the supersaturated solution upon shaking implies a nucleation trigger [19]. We have been focusing on the phenomenon among template crystallizations in which the molecules of the template compound are positioned at the air–solution interface, the air–solution interface becomes the template interface, and the target material crystallizes.

We have investigated the crystallization of glycine at the air–solution interface using the glycine–water–L-leucine (template compound) system as a fundamental study of the crystallization phenomena at the air–solution template interface. Interestingly, our previous study [23] suggested that repulsive force exists between the crystals in the template crystallization at the air–solution interface. It was found that the glycine crystals precipitated at the air–solution interface under conditions with the template were much more uniform in size and had a narrower particle size distribution than those precipitated under conditions without the template. Furthermore, the crystals precipitated at the air–solution interface with the template indicated that the initial crystals were generated at one starting point and then spread out. From these results, the possibility that a repulsive force exists between neighboring crystals, preventing new nucleation at the air–solution template interface, was reported.

Thus, new nucleation is prevented at the template interface after the initial crystalline particles are generated. This means that the total number of crystals does not increase over time. Therefore, it is effective in improving the particle size distribution. However, preventing new nucleation means that the total number of crystals at the template interface at the final is determined solely by the initial crystalline particles. In most cases of crystallization, the total number of crystals is highly dependent on the driving force since a higher driving force increases the nucleation rate and also causes new crystals to be generated over time. On the other hand, considering that the generation of new crystals is prevented at the template interface, the number of crystals does not increase over time, and it can be predicted that it would be difficult to increase the total number of crystals significantly. Therefore, to investigate methods to change the number of crystals at the template interface, it is necessary to observe the crystallization when operations such as changing the driving force are performed.

Therefore, this study aimed to investigate the effects of operations that change the driving force at the air–solution template interface, where new nucleation is prevented, on the number of crystals. Specifically, the effect of changing the supersaturation of the bulk solution and the effect of changing the local supersaturation of the solution near the interface by heating the air–solution interface and promoting solvent evaporation were investigated. In addition, the use of concentration driving force generated by dissolving crystals at the template interface once precipitated was also studied. This phenomenon is discovered when the air–solution interface is heated, a method named “template reset” in this study.

2. Experiment

2.1. Materials

Glycine (guaranteed reagent, 99.0%, FUJIFILM Wako Pure Chemical Corporation, Osaka, Japan) was used as the crystalline substance. Glycine is a substance that increases in solubility with temperature. The template compound was used as L-leucine (guaranteed reagent, 99.0%, Wako Pure Chemical Industries, Ltd.). Distilled water produced in a deionizer (RT-523JO and RG-12, ORGANO Corporation, Tokyo, Japan) was used as the solvent.

2.2. Changing the Supersaturation by Cooling the Bulk Solution

First, the number of crystals precipitated when the supersaturation was changed by cooling the whole bulk solution, an operation that would change the driving force for

the crystallization of the entire solution, was investigated. Figure 1 shows a schematic diagram of the experimental apparatus. However, a heater was not used in this experiment. A glycine-saturated aqueous solution was prepared at 323 K containing L-leucine (1.0×10^{-4} mol/mL-H_2O). A petri dish (29 mm in diameter) placed on a cooling cell was cooled by cooling water from a thermostat bath in a glove box. During the experiment, the cooling water was kept at 293 K, 288 K, 283 K, and 278 K for each batch to achieve a temperature difference (ΔT) of 30 K, 35 K, 40 K, and 45 K with the saturated solution. The glove box was filled with dry air. The air–solution interface was generated when the prepared solutions were fed into a petri dish. Throughout all batches of this study, the amount of solution fed into a petri dish was approximately 2 g. The crystalline particles of glycine precipitated at the air–solution interface in each batch were observed with the optical microscope.

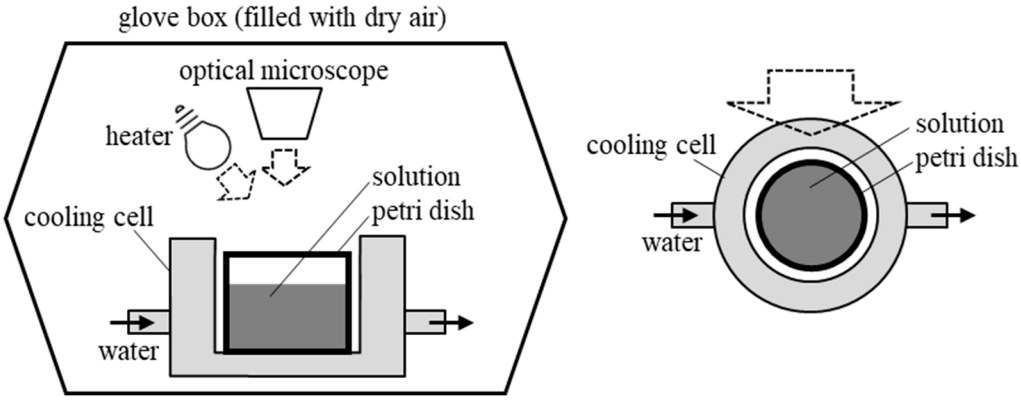


Figure 1. Experimental apparatus.

2.3. Changing the Local Supersaturation by Heating the Template Interface

The number of crystals precipitated when the local supersaturation, due to promoted solvent evaporation, was changed by heating the solution near the air–solution interface as an operation to change the driving force near the interface where the crystals precipitate was investigated. A schematic diagram of the experimental apparatus is shown in Figure 1. A glycine-saturated aqueous solution was prepared at 308 K containing L-leucine (1.0×10^{-4} mol/mL-H_2O). During the experiment, a petri dish (29 mm diameter) in a glove box filled with dry air was cooled with 288 K cooling water (ΔT = 20 K) from a thermostat bath. When the solution was fed into the petri dish and the air–solution interface was generated, a heater started heating the solution near the interface. The input power (I_W = 0, 10, 20, 30, 35, 40, and 50 W) of the incandescent bulbs used as heaters was changed with an electrical transformer. The heater and a petri dish were placed in the same position throughout all experiments. The amount of solution fed was approximately 2 g. The crystalline particles of glycine precipitated at the air–solution interface in each batch were observed with the optical microscope.

2.4. Changing the Local Supersaturation by Temporarily Heating the Interface and Dissolving the Crystals (Template Reset Operation)

The number of crystals precipitated when the local supersaturation was changed by an operation in which the concentration driving force near the template interface was changed by dissolving the crystals at the template interface once precipitated was investigated. Specifically, after the precipitation of crystalline particles, the solution near the interface was temporarily heated to dissolve the crystals. The solution was then cooled again, and crystals were precipitated again at the template interface. Based on the previous study [19], the formation of the new template interface on shaking is a nucleation trigger; shaking and other operations were also applied in this study. The operation of producing a solution near the interface where the crystals were dissolved by temporarily heating the air–solution

interface was named "template reset", and the number of crystals precipitated before and after the template reset operation was investigated.

Figure 1 shows a schematic diagram of the experimental apparatus. The glycine-saturated aqueous solution was prepared at 308 K containing L-leucine (1.0×10^{-4} mol/mL-H_2O). During the experiment, a petri dish (29 mm diameter) was cooled with 288 K cooling water (ΔT = 20 K) from a thermostat bath. An incandescent bulb with I_W = 50 W was used as a heater. Multiple experiments were performed with different cooling and heating times and air conditions. Experimental conditions are summarized in Table 1. In Run 1, an air–solution interface was generated by feeding the solution into a petri dish in a glove box filled with dry air. After cooling for 20 min, the solution was heated near the interface. The heating started, and 20 min later, the heater was turned off and the solution was shaken to recrystallize. From Run 2 to Run 5, the heating time and the operation to recrystallize are different, respectively. From Run 6 to Run 8, experiments were carried out in ambient air, with shorter cooling times and different heating times. The heater and a petri dish were placed in the same position throughout all experiments. The amount of solution fed was approximately 2 g. The crystalline particles of glycine precipitated at the air–solution interface in each batch were observed with the optical microscope.

Table 1. Summary of experimental conditions for performing the template reset operation.

Run No.	Air Condition	Cooling Time before Template Reset (min)	Heating Time (min)	Operation after Heating	Cooling Time after Template Reset (min)
1	dry air	20	20	shaken	20
2	dry air	30	10.5	vibrated	30
3	dry air	30	15	solution dripped	30
4	dry air	30	5.75	vibrated	30
5	dry air	30	17	air sent	30
6	ambient air	10	2.33	shaken	10
7	ambient air	10	3.17	shaken	10
8	ambient air	10	2.33	shaken	10

Since the crystals are dissolved by the template reset operation, the temperature of the solution near the air–solution interface is considered to be higher. Therefore, the difference in temperature between the solution near the interface and the bulk solution was verified. To investigate changes in solution temperature during solution cooling and temporarily heating the interface, the solution temperature was recorded continuously using a thermal logger (LR5021, Hioki E.E. Corporation, Nagano, Japan). Solution temperatures at two different locations in the petri dish, near the interface and at the bottom of the petri dish, were measured simultaneously by holding thermocouples in place. The experimental condition was the same as in Run 1, but the air was ambient air.

2.5. Analysis Method

In this study, the number of crystals per unit area is defined as nucleation density D_N (crystals/mm^2), and D_N (crystals/mm^2) is used to evaluate the number of crystals at the air–solution template interface. The presence of L-leucine results in pyramidal glycine crystals whose basal plane $(0\bar{1}0)$ faces are exposed to air; therefore, the crystallographic axes must be considered [24]. The length along the *a* axis L_a and the length along the *c* axis L_c were measured considering the crystallographic axis, as shown in Figure 2, to evaluate the average size and size distribution of the precipitated crystalline particles.

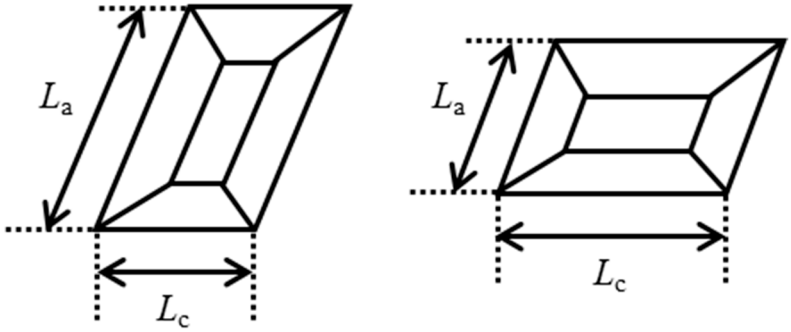


Figure 2. Schematic diagram of the length along the *a* axis L_a and the length along the *c* axis L_c of a glycine crystal at the air–solution template interface.

3. Results and Discussion

3.1. The Effect of Changing the Supersaturation by Cooling the Bulk Solution on the Number of Crystals

Cooling the prepared saturated solution can generate supersaturation, the driving force for crystallization, in the whole bulk solution. Changing the temperature of the cooling water should also be possible for changing the supersaturation. Therefore, the effect on the number of crystals was investigated by observing the crystalline particles precipitated by changing the supersaturation due to cooling the bulk solution. The temperature difference (ΔT) between the saturated solution and the cooling water temperature was defined as the supersaturation of the bulk solution. Figure 3 shows optical photomicrographs of glycine crystals precipitated under different conditions when the supersaturation ΔT of the bulk solution was changed. All images were taken 30 min after feeding the saturated solution, and the nucleation density D_N (crystals/mm^2) was determined from each optical photomicrograph.

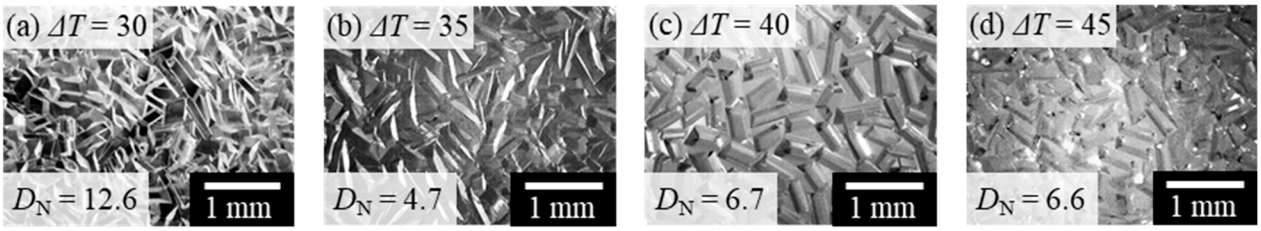


Figure 3. Optical photomicrographs of crystals precipitated at different supersaturation ΔT of the bulk solution.

In all the experiments in this study, there was no significant difference in the particle size of the crystalline particles precipitated on the same air–solution interface in each independent batch. This suggests that even under the conditions of this study, new nucleation at the template interface was prevented, as in previous studies. Figure 3 shows that D_N did not monotonically increase by increasing the solution's supersaturation due to the temperature difference (ΔT) between the bulk solution and the cooling water. In addition, when ΔT was large, crystals were observed to precipitate not only at the template interface but also in the bulk solution, indicating that a simple increase in ΔT is not achievable to increase the D_N at the template interface. Since the target of template crystallization is crystallization at the air–solution interface, it may be required to control the local supersaturation of the solution near the interface.

3.2. The Effect of Changing Local Supersaturation by Heating the Interface on the Number of Crystals

This study's template crystallization precipitates crystals at the air–solution interface. Therefore, if the local supersaturation near the air–solution interface, which is the nucleation

field, can be changed, the number of crystals may be affected. The local supersaturation of the solution near the interface was considered to be changed by promoting solvent evaporation. Solvent evaporation should be able to be promoted by heating the interface. Therefore, while the bulk solution was cooled as usual (ΔT = 20), the air–solution interface was heated to promote solvent evaporation and change the local supersaturation. The effect on the number of crystals was investigated by observing the precipitated crystalline particles. Considering that the local supersaturation can be changed by changing the input power I_W [W] of the heater, the experiment was organized by the value of I_W. Optical photomicrographs of the glycine crystals precipitated under the respective conditions are shown in Figure 4. All images were taken 30 min after feeding the saturated solution, and the nucleation density D_N (crystals/mm^2) was determined from each optical photomicrograph.

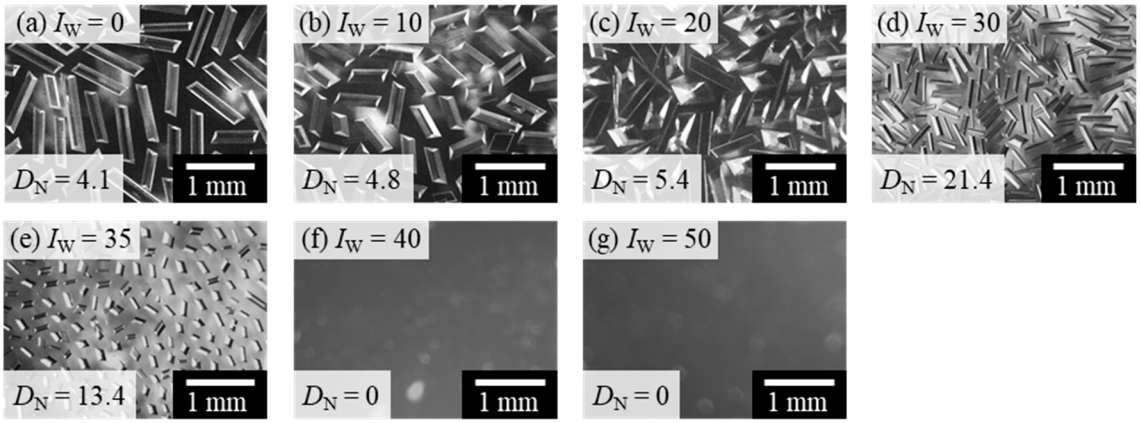


Figure 4. Optical photomicrographs of crystals are precipitated when the local supersaturation is changed by changing the input power I_W.

From the results in Figure 4, D_N was close to values from Figure 4a–c. As I_W increased further, D_N increased in Figure 4d but decreased in Figure 4e. As I_W was further increased in Figure 4f,g, crystals were precipitated at the template interface at the beginning, but the once-precipitated crystals were observed to dissolve. Then, after 30 min, no crystals remained, and D_N = 0. Thus, simply increasing I_W to promote solvent evaporation limited increasing the number of crystals.

The above results show that the number of crystals could not significantly increase even when heating was applied to the air–solution interface to generate local supersaturation due to solvent evaporation. However, the possibility that a local concentration driving force is generated only near the interface due to the dissolution of crystals precipitated at the template interface, which was found when the air–solution interface was heated, was also considered. Therefore, the operation to dissolve the precipitated crystals at the template interface was named "template reset", and the effect of this operation on the number of crystals at the template interface was investigated further.

3.3. The Effect of Changing Local Supersaturation by Template Reset Operation

3.3.1. The Effect on the Number of Crystals

The solution near the interface, where crystals precipitated at the air–solution interface were dissolved by heating the interface, should not only have a temperature gradient but also a concentration gradient. If only the solution near the interface has a high concentration, only the nucleation field can be highly supersaturated, which can affect the number of crystals. Therefore, the local supersaturation was changed by the template reset operation, in which crystals precipitated at the interface by cooling were dissolved by heating the interface. Then, the cooling again, and the crystalline particles precipitated again at the interface, and the effect on the number of crystals were investigated. During the template reset operation, the bulk solution was simultaneously cooled as usual (ΔT = 20). For each

experimental condition, the nucleation density D_N (crystals/mm^2) of the precipitated crystalline particles before and after the template reset operation was determined, and the results are summarized in Table 2. Optical photomicrographs of the glycine crystals precipitated before and after the template reset under the conditions of Run 1 to Run 3 are also shown in Figure 5.

Table 2. Nucleation density D_N results of the crystalline particles precipitated before and after the template reset operation.

Run No.	D_N (Crystals/mm^2) before Template Reset	D_N (Crystals/mm^2) after Template Reset
1	14.7	41.2
2	10.5	28.7
3	1.5	4.6
4	5.9	13.3
5	12.3	27.9
6	20.4	42.7
7	5.7	16.4
8	13.8	28.1

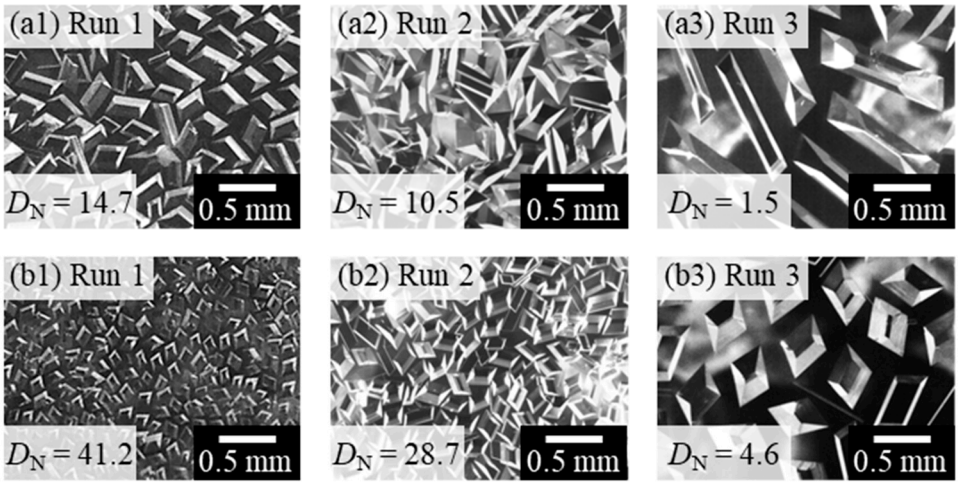


Figure 5. Optical micrographs of crystals precipitated (**a1**–**a3**) before and (**b1**–**b3**) after the template reset operation.

Table 2 and Figure 5 show that the template reset operation at the template interface, which prevents new nucleation, increased D_N compared to before the operation. This suggests that the number of crystals increased due to the local supersaturation of the solution near the interface, the nucleation field, by the template reset operation, in which the crystals precipitated at the interface are dissolved and then re-precipitated. Observation of crystalline particles precipitated by template reset under various conditions suggested the possibility of a relation between D_N before and after the template reset operation. The nucleation density D_N (crystals/mm^2) results in Table 2 are plotted on the chart shown in Figure 6 to investigate the relation between the number of crystals before and after the template reset operation.

Figure 6 shows that D_N increased about 2.3 times after the template reset operation compared to before the operation. This suggests a proportional relation between D_N before and after the template reset operation despite the recrystallization under various conditions. Therefore, the relation shown in Figure 6 indicates that the number of crystals can increase from that of before the operation by performing a template reset operation that changes the local supersaturation using the dissolution of crystals. Thus, it was clarified that the template reset operation is an effective method to increase the number of crystals at the template interface.

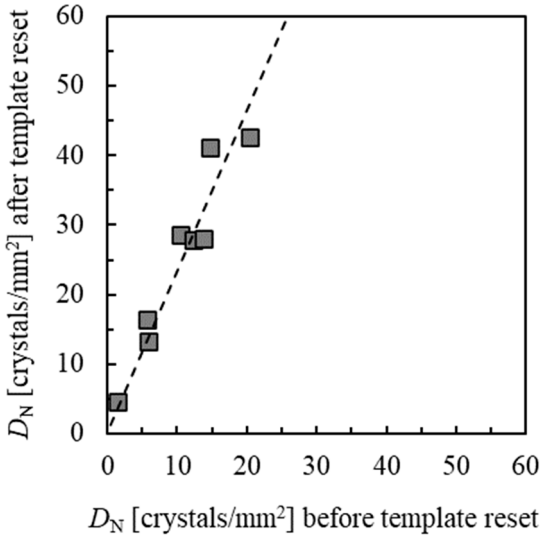


Figure 6. D_N before and after template reset operation.

3.3.2. The Effect on the Size Distribution of Crystalline Particles

Comparing the crystal appearance before and after the template reset operation in Figure 5, the increase in the number of crystals also affects the particle size of the crystalline particles. To evaluate the changes in the crystalline particles' properties before and after the template reset operation, the changes in length L_a and L_c were investigated at three sampling times, each before and after the template reset operation in Run 1. The lengths L_a and L_c were measured over 100 at each sampling time, with the first cooling time before the template reset operation as t_{before} ● and the subsequent cooling time after the operation as t_{after} ◆, and the results are shown in Figure 7a. Based on the *a* axis, *c* axis, and acute angle $\theta = 68.4°$ of the glycine crystal, the particle size was estimated as an equivalent spherical diameter, and the particle size distribution at each sampling time is shown in Figure 7b.

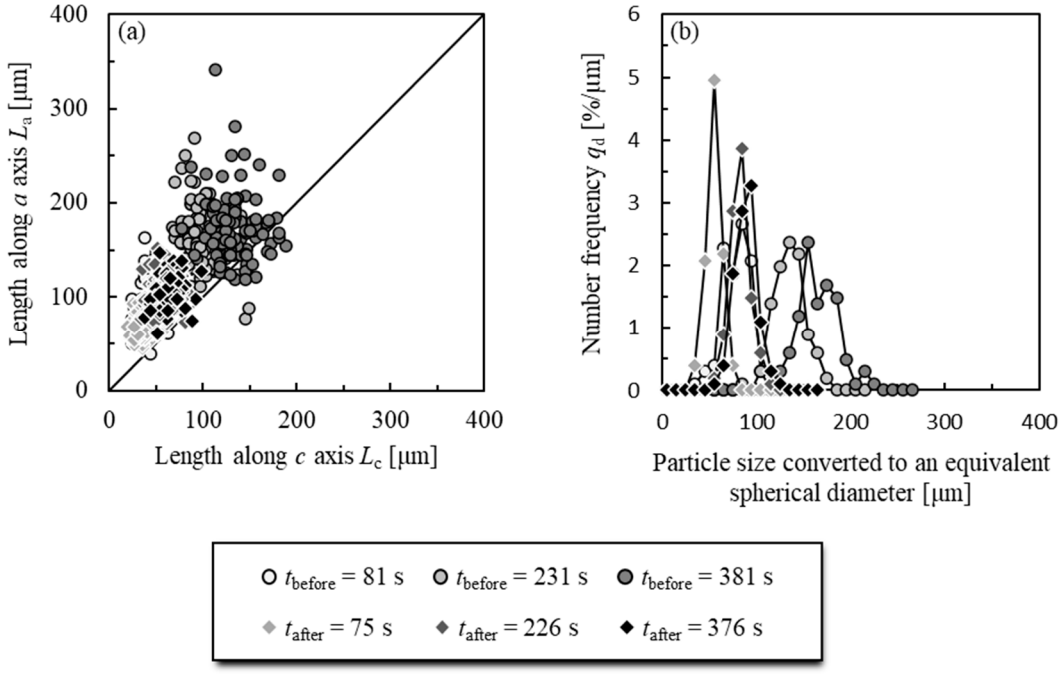


Figure 7. Changes in (**a**) the relation between length L_a and L_c and (**b**) the particle size distribution before and after the template reset operation.

Figure 7a shows that in the conventional template crystallization before the template reset operation, the particle size increased significantly as the cooling time passed, and the aspect ratio variation also increased. In contrast, after the template reset operation, the increase in particle size was smaller, and the variation was also reduced. The average particle size at the time points of t_{before} = 381 s and t_{after} = 376 s was determined, and it was 166.0 μm before the template reset operation, while it was 88.5 μm after the operation, a decrease of about half. Figure 7b shows that the particle size distribution remained broad and shifted before the template reset operation, while it remained sharper after the template reset operation. The distribution width (standard deviation) of the particle size distribution at t_{before} = 381 s and t_{after} = 376 s was determined to be 19.8 μm before the template reset operation, while it was 11.6 μm after the operation, a decrease of about 0.6 times, indicating an improvement. From these results, it can be inferred that the length of the nucleation period was even shorter at the interface after the template reset operation. From the above results, it was considered that the solution near the interface after the template reset was higher than the saturation concentration of the bulk solution because the crystals were dissolved, which was considered to be the reason for the increase in the number of crystals. Therefore, the temperature difference between the bulk solution and the solution near the interface was verified.

3.3.3. Change in Solution Temperature during Template Reset Operation

A series of solution temperature changes in the experiment with the template reset operation were measured simultaneously at two locations: near the air–solution interface, the nucleation field, and the bulk solution at the bottom of the petri dish. The results are shown in Figure 8.

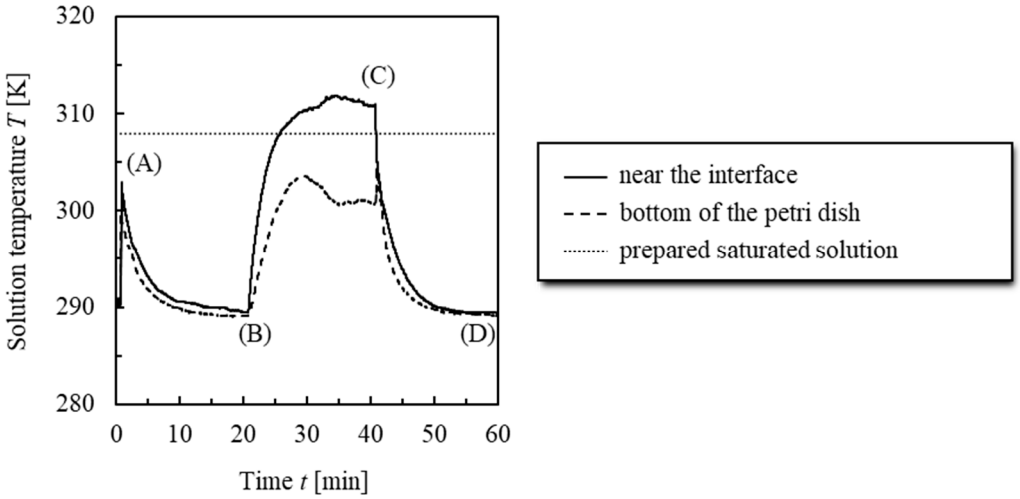


Figure 8. The change over time in temperature of solutions near the interface and at the bottom of the petri dish in the experiment with the template reset operation.

From Figure 8, the solution temperature decreased immediately after the prepared saturated solution was fed into the petri dish (A). There was no significant difference in temperature between the solution near the interface and the solution at the bottom of the petri dish. About 10 min after starting to cool, the solution cooled to around the temperature of the cooling water. Just before heating was started, the solution at the bottom of the petri dish was 289.3 K and the solution near the interface was 289.7 K (B). When heating was started above the interface, the solution temperature increased (B). In particular, the temperature of the solution near the interface immediately increased and exceeded 308 K, the saturation temperature of the prepared saturated solution. At the end of heating, the temperature of the solution at the bottom of the petri dish was 300.6 K, while that near the interface was 310.2 K, a difference of 9.6 K (C). The temperature of the solution near

the interface after template reset was 2.2 K higher than the saturation temperature of the prepared saturated solution. From these results, it is clear that a temperature gradient was generated near the interface, and considering the phenomenon of dissolution of the crystals, a concentration gradient was also generated. In the end, the solution at the bottom of the petri dish and the solution near the interface were cooled to around the cooling water temperature (D).

The solution has no concentration gradient just by preparing a saturated solution. However, when crystals precipitated at the interface are dissolved by heating, the concentration near the interface increases and a concentration gradient is considered to be generated. High supersaturation is generated near the interface when the temperature is cooled with this concentration gradient under no-agitation conditions. Indeed, Figure 8 shows that the temperature of the solution near the interface after template reset was higher than that of the solution at the bottom of the petri dish and also higher than the prepared saturated solution. The solution near the interface should be the saturated concentration at this higher temperature. Therefore, the crystallization driving force is considered higher than in the prepared saturated solution. In this study, the phenomenon at the interface was observed when the template reset was performed. But when the template reset operation is performed, the solution temperature increases and then decreases, which can be likened to the process of making a thermal history. In the case of thermal history as well, a product with a narrow particle size distribution can be obtained by dissolving crystals precipitated by cooling crystallization by raising the solution temperature and then recrystallizing by lowering the temperature. The narrower particle size distribution of the product can be considered evidence of a shorter length of the nucleation period. In a previous study, dissolving the precipitated crystals and then recrystallizing them significantly shortened the induction time and obtained a product with a narrow particle size distribution, which was explained based on the history of the solution structure [25]. Since the phenomenon of change in particle size distribution similar to that observed in the study using the thermal history was also confirmed in this study, this study may have obtained results that support the elucidation of phenomena related to the thermal history.

From the above results, it was found that, at the air–solution template interface where new nucleation is prevented, a novel template reset operation generates a high local supersaturation condition only near the interface, resulting in a significant increase in the number of crystals and an improvement in the particle size distribution.

4. Conclusions

This study investigated the effects of operations that change the driving force at the air–solution template interface, where new nucleation is prevented, on the number of crystals at the interface. As a result, D_N did not monotonically increase even when the supersaturation of the solution due to the temperature difference ΔT between the bulk solution and the cooling water was increased. Then, the local supersaturation of the solution near the interface was changed by heating the air–solution interface and promoting the evaporation of the solvent. As a result, increasing I_W and generating local supersaturation by simply promoting solvent evaporation limited increasing the number of crystals.

However, when I_W was large, crystals once precipitated at the air–solution interface dissolved, suggesting the possibility that the local concentration driving force was generated only near the interface. Therefore, the solution near the interface was temporarily heated to dissolve the crystals by the named "template reset" operation, and then, the crystals were precipitated again. As a result, the D_N was increased more than twice compared to before the template resetting operation. After the template reset operation, the average particle size of the crystalline particles decreased, and the particle size distribution became sharper, indicating that the template reset operation also affected the properties of the crystalline particles. In addition, the template reset operation is similar to the making of the thermal history, and a particle size distribution change phenomenon similar to that observed in the thermal history application study was confirmed.

These results indicate that the number of crystals significantly increases, and the particle size distribution improves at the air–solution template interface, where new nucleation is prevented, when the local supersaturation is changed by the operation that changes the concentration driving force near the interface by dissolving the crystals once precipitated. The results of this study are expected to provide a basis for controlling the number of crystals at the air–solution interface as a fundamental study of the crystallization phenomena in template crystallization, which is promising for the development of crystalline materials in the future.

Author Contributions: Conceptualization, B.-U.T., S.A. and H.T.; methodology, B.-U.T., S.A. and H.T.; validation, B.-U.T.; formal analysis, B.-U.T.; investigation, B.-U.T.; data curation, B.-U.T.; writing—original draft preparation, B.-U.T.; writing—review and editing, S.A. and H.T.; visualization, B.-U.T.; supervision, H.T.; project administration, H.T.; funding acquisition, B.-U.T. All authors have read and agreed to the published version of the manuscript.

Funding: This research was funded by JSPS KAKENHI grant number JP23KJ0860.

Data Availability Statement: The data presented in this study are available upon request from the corresponding author due to privacy.

Conflicts of Interest: The authors declare no conflicts of interest.

References

1. Lei, C.; Dong, Z.; Martinez, C.; Martinez-Triguero, J.; Chen, W.; Wu, Q.; Meng, X.; Parvulescu, A.N.; De Baerdemaeker, T.; Muller, U.; et al. A Cationic Oligomer as an Organic Template for Direct Synthesis of Aluminosilicate ITH Zeolite. *Angew. Chem. Int. Ed. Engl.* **2020**, *59*, 15649–15655. [CrossRef]
2. Chouat, N.; Bensafi, B.; Djafri, F. Post-synthesis fluoride treatment of Analcime zeolite synthesized using a novel organic template. Crystalline, textural, and acid study. *Res. Chem. Intermed.* **2021**, *48*, 491–503. [CrossRef]
3. Verma, V.; Mitchell, H.; Errington, E.; Guo, M.; Heng, J.Y.Y. Templated Crystallization of Glycine Homopeptides: Experimental and Computational Developments. *Chem. Eng. Technol.* **2023**, *46*, 1271–1278. [CrossRef]
4. Manghnani, P.N.; Schenck, L.; Khan, S.A.; Doyle, P.S. Templated Reactive Crystallization of Active Pharmaceutical Ingredient in Hydrogel Microparticles Enabling Robust Drug Product Processing. *J. Pharm. Sci.* **2023**, *112*, 2115–2123. [CrossRef]
5. Verma, V.; Bade, I.; Karde, V.; Heng, J.Y.Y. Experimental Elucidation of Templated Crystallization and Secondary Processing of Peptides. *Pharmaceutics* **2023**, *15*, 1288. [CrossRef] [PubMed]
6. Sundareswaran, S.; Karuppannan, S. Isolation and Stabilization of the Metastable Form-II Polymorph of Vanillin. *Chem. Eng. Technol.* **2022**, *45*, 687–693. [CrossRef]
7. Gerard, C.J.J.; Briuglia, M.L.; Rajoub, N.; Mastropietro, T.F.; Chen, W.; Heng, J.Y.Y.; Di Profio, G.; Ter Horst, J.H. Template-Assisted Crystallization Behavior in Stirred Solutions of the Monoclonal Antibody Anti-CD20: Probability Distributions of Induction Times. *Cryst. Growth Des.* **2022**, *22*, 3637–3645. [CrossRef] [PubMed]
8. Zhang, J.; Lou, B.; Qin, X.; Li, Y.; Yuan, H.; Zhang, L.; Liu, X.; Zhang, Y.; Lu, J. Using Amphiphilic Polymer Micelles as the Templates of Antisolvent Crystallization to Produce Drug Nanocrystals. *ACS Omega* **2022**, *7*, 21000–21013. [CrossRef] [PubMed]
9. Zheng, Z.; Yang, Y.; Chen, D.; Wang, S.; Li, Q.; Zhang, Z.; Li, W.; Chen, B.; Wang, W.J.; Liu, P. Engineering hollow covalent organic framework particle through self-templated crystallization. *J. Polym. Sci.* **2023**, *62*, 1698–1705. [CrossRef]
10. Banerjee, M.; Brettmann, B. Combining Surface Templating and Confinement for Controlling Pharmaceutical Crystallization. *Pharmaceutics* **2020**, *12*, 995. [CrossRef]
11. Bora, M.; Hsu, M.N.; Khan, S.A.; Doyle, P.S. Hydrogel Microparticle-Templated Anti-Solvent Crystallization of Small-Molecule Drugs. *Adv. Healthc. Mater.* **2022**, *11*, e2102252. [CrossRef] [PubMed]
12. Minecka, A.; Tarnacka, M.; Jurkiewicz, K.; Zakowiecki, D.; Kaminski, K.; Kaminska, E. Mesoporous Matrices as a Promising New Generation of Carriers for Multipolymorphic Active Pharmaceutical Ingredient Aripiprazole. *Mol. Pharm.* **2023**, *20*, 5655–5667. [CrossRef] [PubMed]
13. Akkineni, S.; Doerk, G.S.; Shi, C.; Jin, B.; Zhang, S.; Habelitz, S.; De Yoreo, J.J. Biomimetic Mineral Synthesis by Nanopatterned Supramolecular-Block Copolymer Templates. *Nano Lett.* **2023**, *23*, 4290–4297. [CrossRef] [PubMed]
14. Davila-Hernandez, F.A.; Jin, B.; Pyles, H.; Zhang, S.; Wang, Z.; Huddy, T.F.; Bera, A.K.; Kang, A.; Chen, C.L.; De Yoreo, J.J.; et al. Directing polymorph specific calcium carbonate formation with de novo protein templates. *Nat. Commun.* **2023**, *14*, 8191. [CrossRef] [PubMed]
15. Butto, N.; Cotrina Vera, N.; Díaz-Soler, F.; Yazdani-Pedram, M.; Neira-Carrillo, A. Effect of Chitosan Electrospun Fiber Mesh as Template on the Crystallization of Calcium Oxalate. *Crystals* **2020**, *10*, 453. [CrossRef]
16. Liu, J.; Yu, Y.; Liu, J.; Li, T.; Li, C.; Zhang, J.; Hu, W.; Liu, Y.; Jiang, L. Capillary-Confinement Crystallization for Monolayer Molecular Crystal Arrays. *Adv. Mater.* **2022**, *34*, e2107574. [CrossRef] [PubMed]

17. Liang, X.; Xue, S.; Yang, C.; Ye, X.; Wang, Y.; Chen, Q.; Lin, W.; Hou, Y.; Zhang, G.; Shalom, M.; et al. The Directional Crystallization Process of Poly (triazine imide) Single Crystals in Molten Salts. *Angew. Chem. Int. Ed. Engl.* **2023**, *62*, e202216434. [CrossRef] [PubMed]
18. Wu, Z.; Wu, Y.; Yang, L.; Zuo, X.; Wang, Z.; Yan, Y.; Li, W.; Chang, D.; Guo, Y.; Mo, X.; et al. Template-Assisted Fabrication of Single-Crystal-Like Polymer Fibers for Efficient Charge Transport. *Adv. Fiber Mater.* **2023**, *5*, 2069–2079. [CrossRef]
19. Yamamoto, H.; Takiyama, H. Production of organic micro-crystals by using templated crystallization as nucleation trigger. *J. Cryst. Growth* **2013**, *373*, 69–72. [CrossRef]
20. Li, H.; Wang, L.; Wei, Y.; Yan, W.; Feng, J. Preparation of Templated Materials and Their Application to Typical Pollutants in Wastewater: A Review. *Front. Chem.* **2022**, *10*, 882876. [CrossRef]
21. Tepale, N.; Fernández-Escamilla, V.V.A.; Carreon-Alvarez, C.; González-Coronel, V.J.; Luna-Flores, A.; Carreon-Alvarez, A.; Aguilar, J. Nanoengineering of Gold Nanoparticles: Green Synthesis, Characterization, and Applications. *Crystals* **2019**, *9*, 612. [CrossRef]
22. Tian, W.; Ogunyinka, O.; Oretti, C.; Bandulasena, H.C.H.; Rielly, C.; Yang, H. Protein crystallisation with gas microbubbles as soft template in a microfluidic device. *Mol. Syst. Des. Eng.* **2023**, *8*, 1275–1285. [CrossRef]
23. Suzuki, H.; Takiyama, H. Observation and evaluation of crystal growth phenomena of glycine at the template interface with L-leucine. *Adv. Powder Technol.* **2016**, *27*, 2161–2167. [CrossRef]
24. Weissbuch, I.; Addadi, L.; Berkovitch-Yellin, Z.; Gati, E.; Weinstein, S.; Lahav, M.; Leiserowitz, L. Centrosymmetric crystals for the direct assignment of the absolute configuration of chiral molecules. Application to the .alpha.-amino acids by their effect on glycine crystals. *J. Am. Chem. Soc.* **1983**, *105*, 6615–6621. [CrossRef]
25. Xing, Z.; Igarashi, K.; Morioka, A.; Ooshima, H. Repeated Cooling Crystallization for Production of Microcrystals with a Narrow Size Distribution. *J. Chem. Eng. Jpn.* **2012**, *45*, 5. [CrossRef]

Disclaimer/Publisher's Note: The statements, opinions and data contained in all publications are solely those of the individual author(s) and contributor(s) and not of MDPI and/or the editor(s). MDPI and/or the editor(s) disclaim responsibility for any injury to people or property resulting from any ideas, methods, instructions or products referred to in the content.